Journal of Structural Geology, Vol. 9, No. 4, pp. 403 to 417, 1987
Printed in Great Britain

0191-8141/87 $03.00 + 0.00


# Diagenetic controls on the structural evolution of siliceous sediments in the Golconda allochthon, Nevada, U.S.A.

HANNES K. BRUECKNER,*† WALTER S. SNYDER‡ and MARION BOUDREAU*

* Department of Geology, Queens College of The City University of New York, Flushing, NY 11367, U.S.A.

† Lamont–Doherty Geological Observatory of Columbia University, Palisades, NY 10964, U.S.A.

‡ Department of Geology and Geophysics, Boise State University, Boise, ID 83725, U.S.A.

(*Received* 3 *April* 1986; *accepted in revised form* 10 *November* 1986)

**Abstract**—A model is proposed that links the diagenesis of siliceous sedimentary rocks with deformation to explain the heterogeneous structural fabric of radiolarian cherts in the upper Paleozoic Golconda allochthon of Nevada, U.S.A. Numerous thrust faults slice the cherts into packets, each with a unique set of internal structures. Fold geometries, boudin profiles, pressure-solution features, etc. vary from packet-to-packet and layer-to-layer. Analogous variations in the diagenetically mixed siliceous sediments of the Miocene Monterey Formation, California, suggest the cherts of the Golconda allochthon were similarly mixed when they were deformed.

Radiolarian sediments composed of biogenic silica (opal-A) developed ductile structures and pressure-solution features because of their high porosity, weak lithification and the high solubility of disordered silica. Low-porosity, strongly-lithified, relatively-insoluble quartz cherts, the final product of silica diagenesis, deformed in a brittle fashion and developed fewer pressure-solution features. Diagenetically intermediate CT-cherts and CT-porcelanites exhibited transitional behavior. Mixed diagenetic zones produced structures with layer-by-layer changes in structural style. The dehydration of opal-A and opal-CT helped create the excess pore fluid pressures responsible for thrust faults, hydraulic fractures, dilation breccias and clastic intrusions. The presence of ductile structures and numerous pressure solution features in the oldest cherts of the Havallah sequence suggests that these cherts were deformed while diagenetically immature, possibly within a long-lived upper Paleozoic accretionary prism.

## INTRODUCTION

THE Golconda allochthon of central and northern Nevada was thrust eastward over upper Paleozoic shelf rocks of western North America during the Permo-Triassic Sonoma Orogeny (Silberling & Roberts 1962). It is widely exposed in several ranges (Fig. 1) and includes correlative, chert-rich, ocean-floor assemblages such as the Havallah sequence (Roberts *et al.* 1958), the Schoonover sequence (Miller *et al.* 1984), the Willow Canyon Formation (Laule *et al.* 1981) and the Pablo Formation (Speed 1977a). These units contain Late Devonian to early Late Permian radiolaria, conodonts and fusilinids (Miller *et al.* 1984, Laule *et al.* 1981, Stewart *et al.* 1977, 1986, Snyder & Brueckner unpublished data) and they are separated from coeval, autochthonous units of shallow marine and non-marine origins by the Golconda thrust (Roberts *et al.* 1958). For convenience, we will henceforth use the term Havallah sequence when referring to the rocks within the Golconda allochthon.

The rocks of the Havallah sequence are largely (>50%) siliceous, and range from pure radiolarian ribbon chert to siliceous argillite. Associated, subordinate rocks include siliciclastic, calcarenitic and volcaniclastic turbidites and, locally, chert, volcaniclastic and multilithic slump breccias. Havallah cherts rest depositionally on basaltic rocks of tholeiitic affinity (Snyder 1977, 1978) and this contact is locally associated with mid-ocean ridge-type hydrothermal deposits (Rye *et al.* 1984).

The Havallah sequence was complexly deformed while at relatively low temperatures. We have studied the structural fabric of the Havallah sequence where it is unmetamorphosed in Battle and Edna Mountains and the Sonoma, Tobin and Toquima Ranges (Fig. 1) with particular emphasis on small-scale structures in cherts (Brueckner & Snyder 1985a). Here we deal with an aspect of the chert fabric; the relationship between silica diagenesis and deformation. At low temperatures siliceous sediments undergo a protracted and complicated diagenetic evolution during their conversion to quartz chert. Our studies of the Miocene Monterey Formation of California (Snyder *et al.* 1983) suggest that the rheologies, solubilities and pore-fluid pressures of siliceous sediments change with advancing diagenesis and hence the structures developed in siliceous sediments vary as a function of their diagenetic state.

The first part of this paper reviews the heterogeneous structural fabric of Havallah cherts (further details and illustrations are presented in Brueckner & Snyder 1985a) and attempts to demonstrate that much of this heterogeneity is the result of differences in the rheologies and solubilities of the chert layers themselves rather than to variations in external factors such as strain rate. The second part uses the Monterey Formation as a modern-day analogue to suggest that the Havallah sequence, like the Monterey Formation, was deformed while the siliceous sediments were in variable diagenetic states.

At the end we deal briefly with some of the tectonic and paleogeographic implications of the diagenesis–



SG 9:4-B

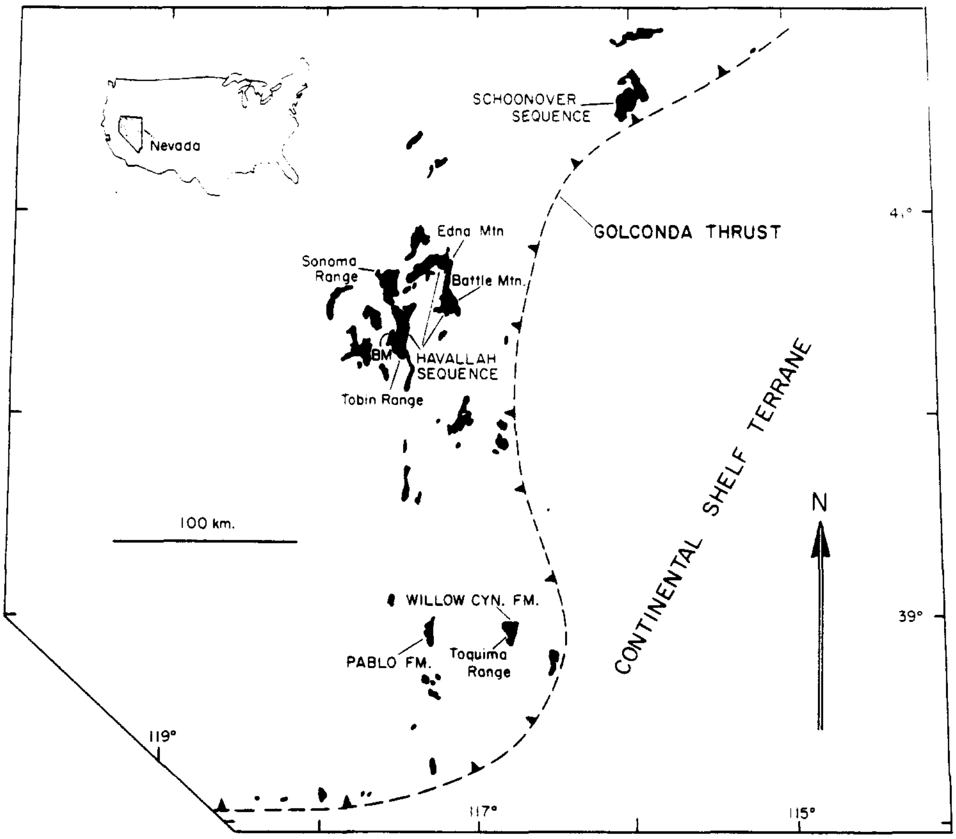


Fig. 1. Index map of Nevada showing the distribution of the Havallah sequence and correlative rocks of the Golconda allochthon. Position of Golconda thrust is generalized. BM refers to the Big Mike massive sulfide mine.

deformation model (see also Siever 1983). The major tectonic problem of the Golconda allochthon is to determine whether it is a far-travelled exotic terrain or whether it was never far from the west coast of Upper Paleozoic North America (see Snyder & Brueckner 1983 and Miller *et al.* 1984 for recent reviews). The diagenesis–deformation model implies that some of the oldest (upper Devonian–lower Mississippian) siliceous packets of the Havallah sequence were deformed within a few tens of millions of years after deposition, well before the classic Permo-Triassic Sonoma orogeny, perhaps within a long-lived and much-travelled accretionary prism. The Sonoma orogeny would then simply mark the time the accretionary prism obducted onto North America.

## STRUCTURE

### *General*

Large-scale thrust faults slice the Havallah sequence into lithotectonic units of different ages and/or lithologies (Ferguson *et al.* 1952, Stewart *et al.* 1977, 1986, Miller *et al.* 1984, Brueckner & Snyder 1985a, Laule *et al.* 1981). The lithotectonic units are cut in turn by numerous internal thrust faults (Stewart *et al.* 1986, Brueckner & Snyder 1985a). These internal thrusts are generally parallel or subparallel to bedding and do not always separate units of different fossil age. Hence they have not been generally recognized. Their presence is indicated by slickensided and cataclastic surfaces and/or by juxtaposed units of different lithology, internal structural fabric or age. They are, at least locally, very numerous (see fig. 3 in Brueckner & Snyder 1985a), with spacings ranging from m to tens of m. The structural units bounded by these thrusts are called tectonic packets.

Tectonic packets contain, or are deformed by, numerous other structures including north–south striking micro-faults, brittle boudins, solution boudins, bed-parallel and bed-normal solution cleavages, at least two sets of north- or south-plunging, east-verging folds, a later set of west-verging folds, hydraulic fractures, crack-seal fractures, dilation breccias and clastic intrusions. Refolded folds, folds cut by thrust faults, folded thrust surfaces, brecciated solution features and other cross-cutting relationships demonstrate a polyphase structural evolution for the Havallah sequence. The relative ages of these structures, based on an idealized chert packet that recorded all Havallah structures, are presented in Table 1 (modified from Brueckner & Snyder 1985a). The ensuing discussion is restricted to those 'internal' structures that developed during or before thrusting ($D_2$ or earlier in Table 1). These structures define a characteristic internal fabric, terminated at the packet boundaries by thrusts, that differ from packet to packet. Each packet has a structural individuality that distinguishes it from neighboring packets. Extreme cases exist where unfolded chert packets are juxtaposed with complexly deformed chert packets.

Table 1. Structural events of an idealized chert packet in the Havallah sequence of north-central Nevada (from Brueckner & Snyder 1985a). No single chert packet records all fabrics

| Event | Fabric elements | Orientation | Comments |
|---|---|---|---|
| $D_0$ | Fractures & qtz-veins, microstylolites ($C_0$), mound structures, dilation breccias? slumps? | Fracture & veins, variable, at high angles to beds. $C_0$ parallels bedding. | Sedimentary loading. Fractures & veins from volume changes during diagenesis. |
| $D_1$ | Solution boudins, microfaults, further formation of microstylolites ($C_1$), isoclinal folds with $C_1$ axial cleavage? | $C_1$ parallel to bedding. Microfaults strike N–S. Boudins form N-plunging maximum. | Early tectonics with bedding-normal loading, some E–W extension. Extreme thinning by solution. |
| $D_2$ | Thrusting, cataclasis, tight to open E-verging folds ($F_2$), solution cleavage ($C_2$), crack-seal fractures, dilation breccias, etc. | Folds parallel boudin axes. $C_2$ at high angles to bedding. Thrusts at very low angles to bedding. | E-directed thrusting (in accretionary prism?). Chert packets juxtaposed. Episodes of high and low pore pressures. |
| | Asymmetric folds ($F_2$A) predate thrusts or refolded. $C_2$ in hinges. | Generally N-plunging hinges. Axial surfaces refolded. | Folds usually tight or chevron, local ductile behavior. |
| | Thrusts, thrust zones, clastic intrusions. | Very low angles to bedding. | Several generations of thrusts. |
| | Asymmetric folds ($F_2$B), concentric, post-thrust. | Generally N-plunging hinges. | Folding more disharmonic than $F_2$A. |
| $D_3$ | Golconda thrust and major internal thrusts. Large asymmetric concentric folds ($F_3$), vergence east. | Folds parallel $D_2$ fold fabric. Major thrusts cut off $D_2$ thrusts. | Permo-Triassic obduction onto North American Craton (Sonoma Orogeny). |
| $D_4$ | Asymmetric, gentle to open concentric folds ($F_4$), vergence west. | Scattered, generally N-plunging. | Possibly related to Mesozoic events. |

*Pressure-solution features*

Nearly every chert sample contains bed-parallel *microstylolites*, which are micron-thick, irregular, discontinuous laminae filled with clay and opaque material (Figs. 2a–d). They are locally stylolitic and abut against partially dissolved radiolaria (fig. 5 in Brueckner & Snyder 1985a). Closely-spaced (mm) anastomosing networks of these laminae are called microstylolite *swarms* and very densely spaced (microns) concentrations are called clay *seams* (Figs. 2a & b). We attribute these features to the dissolution and removal of silica parallel to bedding as a result of bedding-normal loading (Wanless 1979). Although microstylolites are nearly ubiquitous structures, their abundance and spacing vary widely from packet-to-packet, layer-to-layer and within single layers (Figs. 2a, b & d).

Quartz and chalcedony veins that cross-cut microstylolite-rich zones at high angles are strongly crumpled and locally brecciated, whereas they are undeformed where they cross-cut microstylolite-free layers (Figs. 2a and 3c). This relationship suggests that a solubility contrast existed between the quartz in the veins and the silica in the matrix. The soluble matrix thinned by pressure solution whereas the less soluble quartz veins buckled and fractured to accommodate shortening normal to bedding.

Havallah cherts also contain a spaced, stylolitic solution cleavage oriented at high angles to bedding. This cleavage crudely parallels the fold axial surface (Fig. 4b) in the hinge areas of some folds and occurs locally in unfolded chert layers. An example shown in Fig. 2(b) indicates that the upper layer was more soluble than the lower layer during the development of both the bedding-parallel clay seam and the high angle solution cleavage.

*Mound structures* are knobby or moundlike irregularities in the thickness of chert layers (Fig. 2c). They usually have an oblate spheroid shape with the long axes parallel to layering. Many contain curved growth rings of alternating quartz and chalcedony that are concentric to the core of the mound (Fig. 2d). The rings are locally terminated by clay-rich seams indicating some of the mound material had been dissolved.

Mound structures provide important evidence for solubility variations within individual layers. The thin portions of the layers between the mounds in the example shown in Fig. 2(c) contain many more microstylolites than the mounds, and the microstylolites are pinched together in the middle and splayed towards the mounds. This configuration suggests that the far more soluble matrix material between the mounds was thinned by silica removal whereas the relatively insoluble mounds were not.

*Ribbon cherts* or 'bedded cherts' of the Havallah sequence are composed of cm-thick, clay-poor (<20%) chert layers separated by thinner (mm) clay-rich (>80%) zones or 'argillite partings'. We suggest that these chert–argillite couplets are the result of interlayer variations in silica solubility similar to the intralayer variations suggested by the mound structures. The initial localization of clay-rich vs clay-poor layers may have been set during deposition. Layers originally slightly higher in clay than neighboring layers are believed to have been thinned and further enriched in residual clay by bed-parallel pressure solution. Thus the argillite partings are thought to be microstylolite-rich clay seams.

Some microstylolites cut folds, an oriented set of microfaults, and clastic intrusions associated with thrust faults. Thus some, although not necessarily all, of the microstylolite fabric is tectonic, possibly the result of loading by stacked thrust sheets (Brueckner & Snyder 1985a). If the argillite partings are insoluble clay seams, then the 'bedded' or ribbon appearance of Havallah cherts and cherts from other siliceous sequences are

Figures 2–5 appear on the following pages

Fig. 2. Pressure-solution features in siliceous sediments of the Golconda allochthon. (a) Negative print of thin section of chert from Willow Canyon, Toquima Range showing bed-parallel microstylolites (thin white laminae) concentrated as seams. The seams are not parallel to bedding proving they are not sedimentary features. Subvertical antitaxial quartz veins (dark) are relatively straight where microstylolites are rare, but folded and brecciated where they cross and near to the seams. Note accreted, splayed microstylolites where folded quartz vein formed rigid buttresses at top. (b) Positive print of thin section of chert from Water Canyon, Sonoma Range. Two layers are separated by microstylolite-rich solution seam and the upper layer is crossed at a high-angle by stylolitic solution cleavage. (c) Negative print of thin section of two small mounds and intervening matrix from cherts of the Schoonover sequence, Independence Range. The mounds (labeled 'M') have few internal solution features whereas the material between the mounds contains concentrated bed-parallel microstylolites and microstylolite (white). (d) Negative print of thin section of mound from Willow Canyon, Toquima Range, showing relationship between mound growth rings and bed-parallel microstylolite development. Concentric, alternating light (quartz) and dark (chalcedony) bands are growth rings of a mound that started at nucleus (marked 'core') in lower right. Microstylolites (thin, irregular, white laminae) become more abundant away from the nucleus and form seams and swarms near upper boundary.

Fig. 3. (a) Chert layers cut by N–S striking, closely-spaced microfaults, Willow Creek, Battle Mountain. Dip–slip component of motion on the step planes creates a staircase effect (step lines). Microfaults are normally not this closely spaced. The coin is 25 mm in diameter. (b) Profile view of solution-modified step lines from unit C-7, Hoffman Canyon, Tobin Range. Internal laminations (sketched as white dashed lines) show no evidence of ductile extension and necking and are terminated by solution-modified microfaults or solution seams. (c) Negative print of thin section of hinge area of folded mound structures. Four small mounds (M) are internally undeformed and contain few or no pressure-solution features, whereas the matrix material is folded and contains highly concentrated microstylolites (thin white laminae) and solution seams (thicker white zones). Note buckled quartz veins (dark) at upper right. (d) Polished slab showing hinge from Permian cherts, Willow Canyon, Toquima Range. V-Shaped tension gashes opened along the outer surface of the lower layer as it buckled. The layer above was more ductile and sagged into the tension gashes. Vertical black lines in the core mark axial surface microstylolites that indicate inner arc underwent pressure solution during folding. Dotted lines trace sedimentary layering.

Fig. 4. (a) Two adjacent, disharmonically folded chert layers from unit C-5, Hoffman Canyon, Tobin Range. Black lines trace layering. (b) Negative print of thin section showing detail of syncline from the upper layer. Sedimentary layers and bed-parallel microstylolites show subtle to abrupt orientation changes across irregular, solution cleavage surfaces (white traces) that are sub-parallel to the fold axial surface. (c) Negative print of thin section of anticline in lower layer. Laminae and thin bed-parallel microstylolite seams (white) are smoothly curved around the hinge. Note small tension gashes below the seam in the middle. Some faulting occurred in the core. The origin of the irregular, diffuse dark zones is unknown.

Fig. 5. Structures from the siliceous, Miocene Monterey Formation of California. (a) Diagenetic nodule of CT-chert enclosed in opal-A diatomite, Johns-Manville Quarry Road, Lompoc, California. Nodule growth occurred as successive concentric zones converted from opal-A to opal-CT. Note similarity to rings in mound shown in Fig. 2(d). (b) Folded interlayered CT-porcelanite and opal-A diatomite from Sweeny Canyon Road, east of Lompoc, California. The CT-porcelanite layers (P) maintain thickness around the fold hinges and/or are fractured. Ductile diatomite (D) layers flowed into the hinge areas to accommodate room problems created by folding of the porcelanites. (c) Folded thinly-interbedded quartz-chert and CT-chert from Lions Head, California. The quartz-chert (black) has shattered and forms a curved train of straight fragments. The white CT-chert either folded without fracturing or was diagenetically produced after folding to form a cement to the quartz-chert fragments.

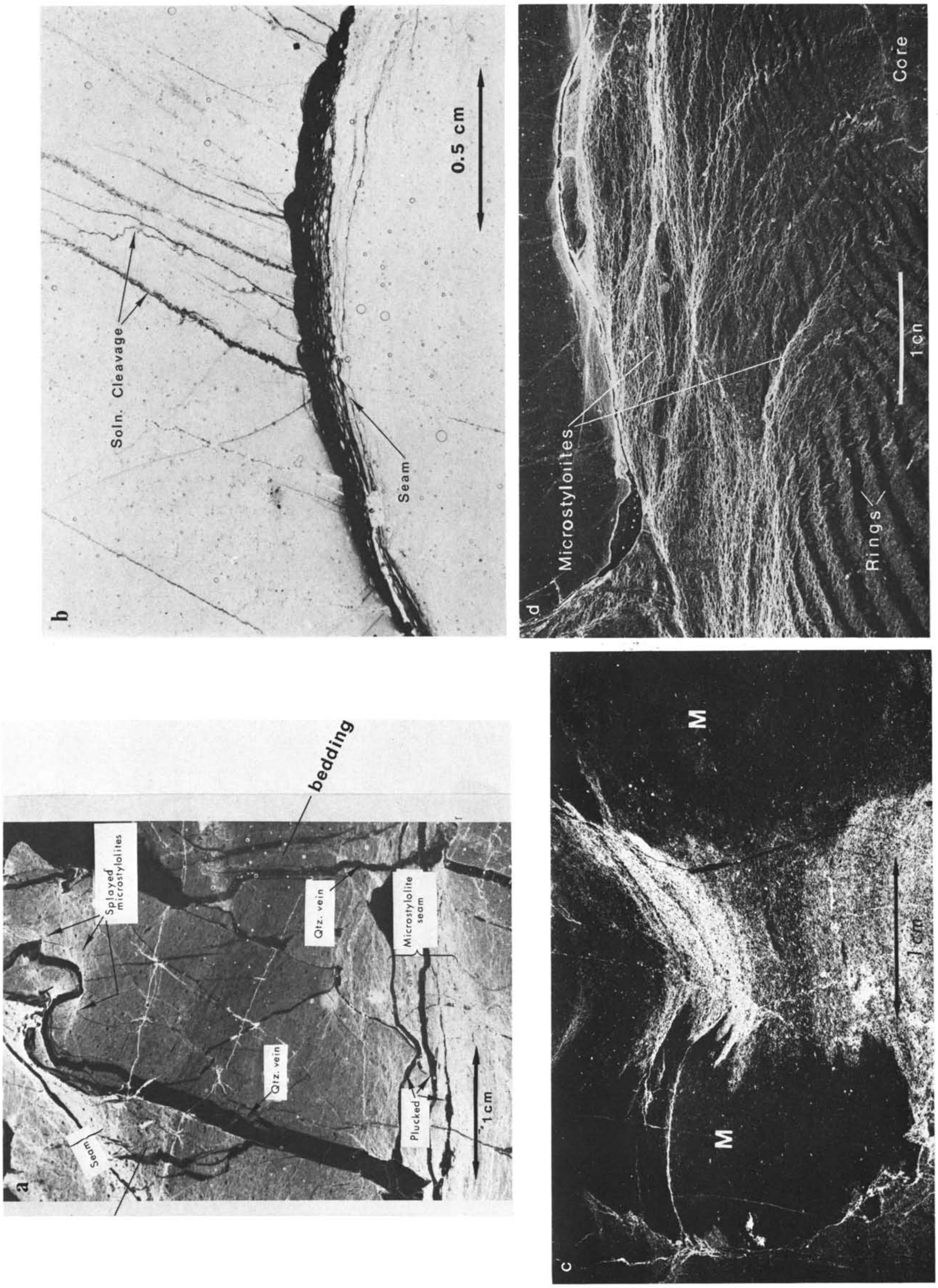
a
Seam
Splayed microstylolites
bedding
Qtz. vein
Qtz. vein
Microstylolite seam
Plucked
1 cm
b
Soln. Cleavage
Seam
0.5 cm
c
M
M
1 cm
d
Microstylolites
Rings
Core
1 cm

Fig. 2.

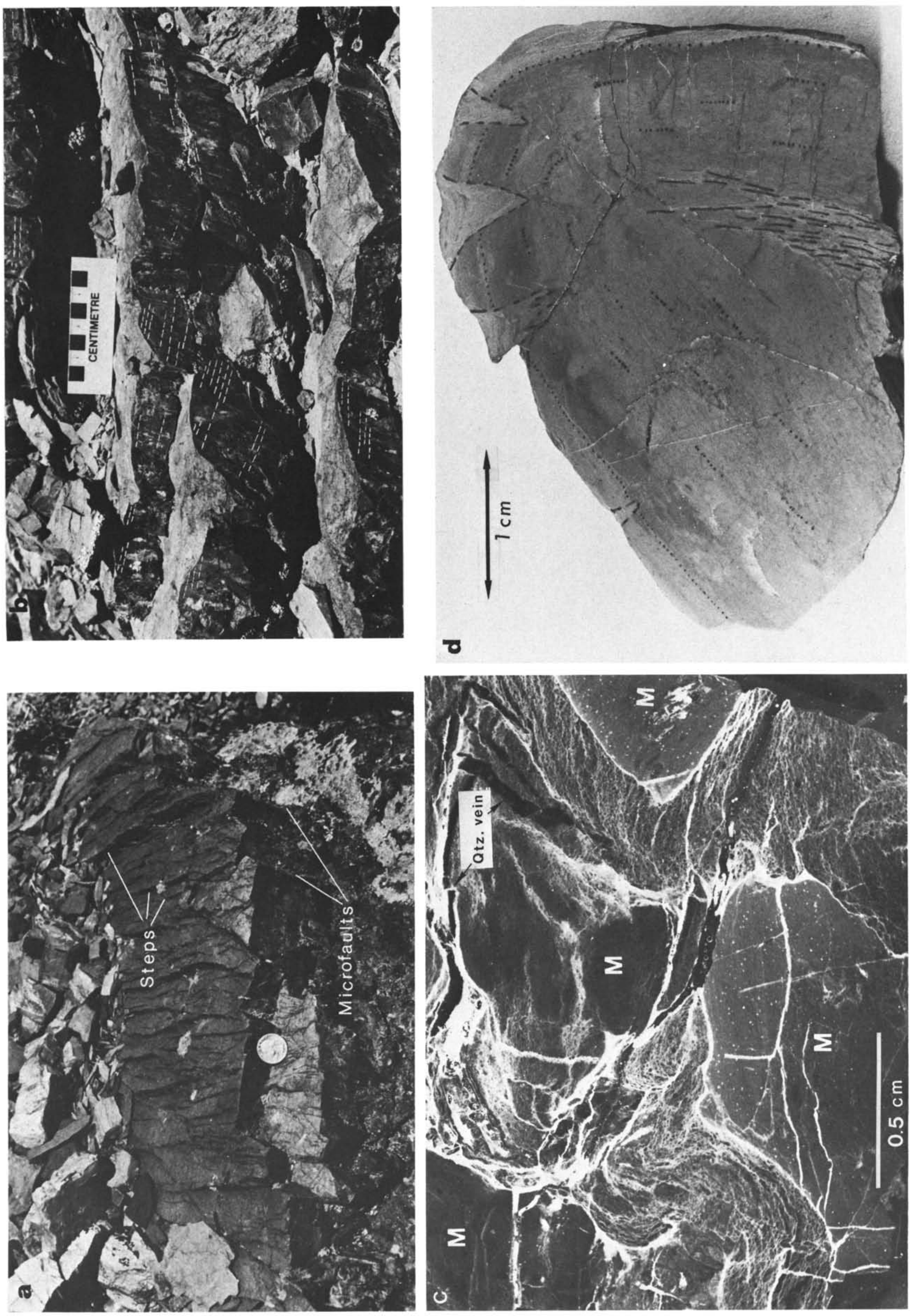


Fig. 3.

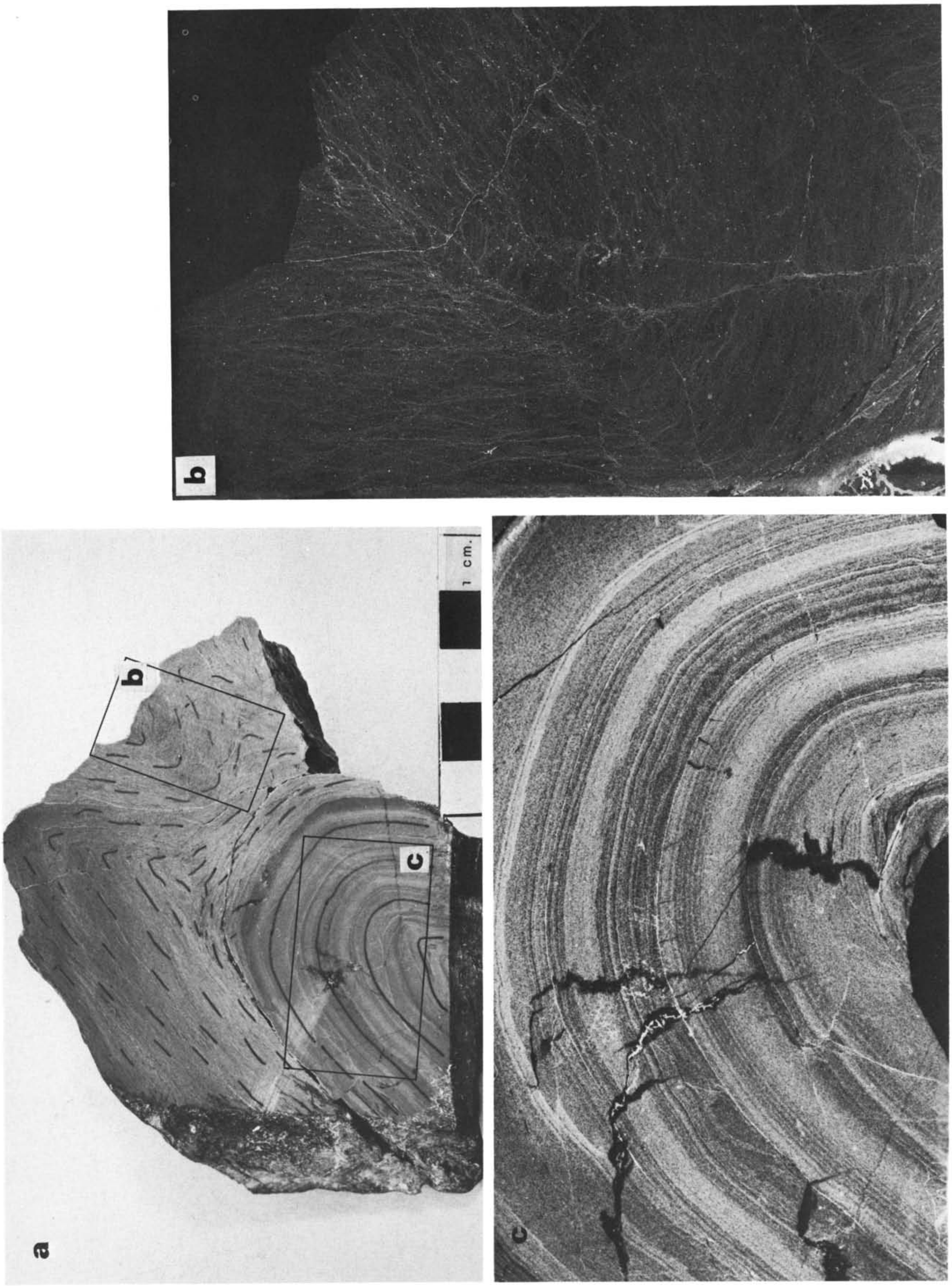


Fig. 4.

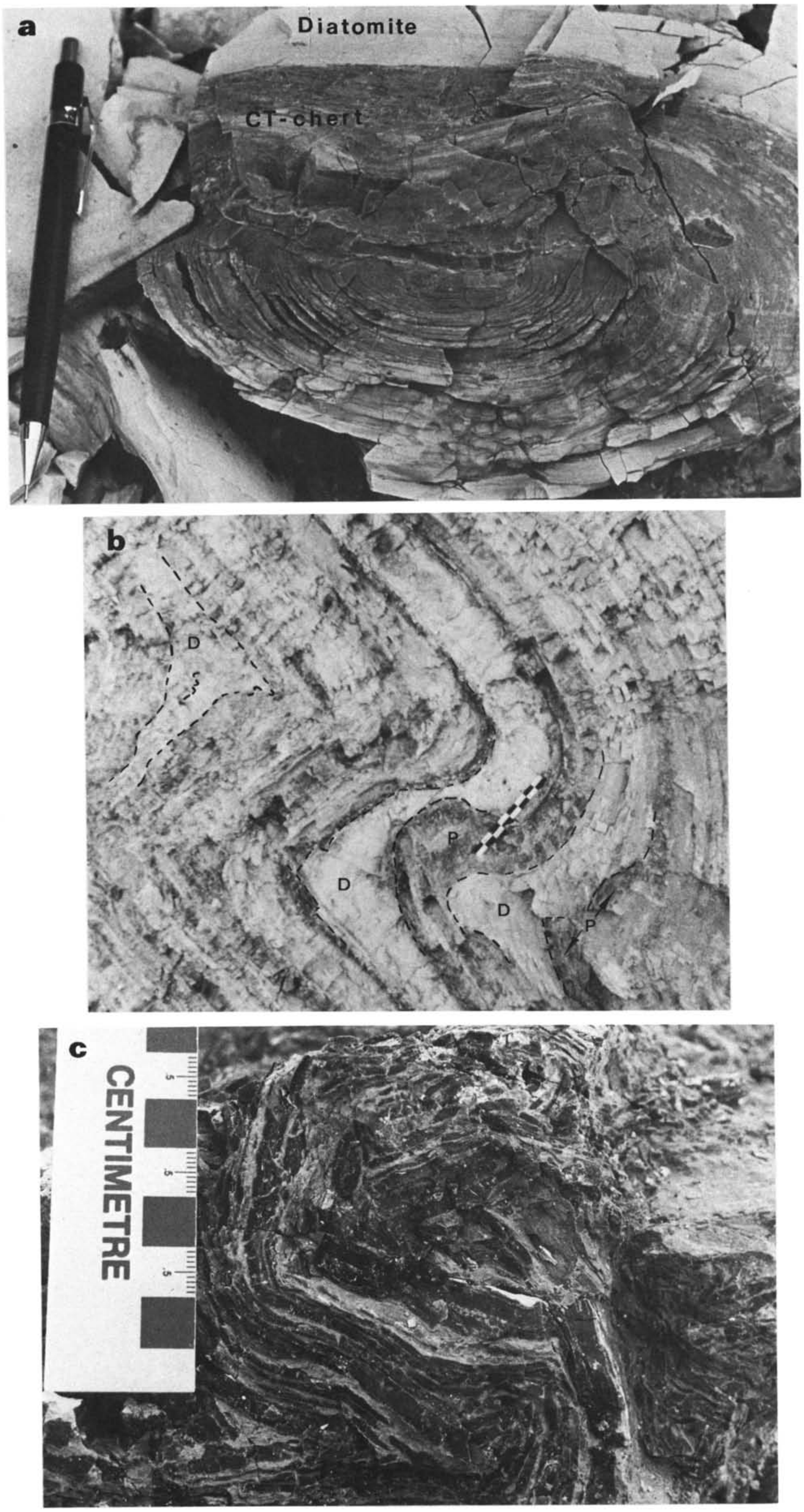


Fig. 5.

partly tectonic, rather than purely depositional, features. This hypothesis could explain the apparent lack of modern ribbon cherts on the floors of major ocean basins (Jenkyns & Winterer 1982).

The development of the planar microstylolite fabric, especially the clay seams, was a significant process in the Golconda allochthon because it created potential slip surfaces for subsequent deformation and strong contrasts in clay content for subsequent pressure solution.

*Oriented microfaults, brittle boudins and solution boudins*

Havallah cherts have a set of spaced (cm–tens of cm) fractures at high angles to bedding that generally display a north–south-striking preferred orientation. These oriented fractures underwent dip–slip motion, but they usually offset a single layer or, at most, two or three chert layers and are terminated in clay seams. The intersection of these fractures with the offset bedding surfaces creates little steps (Fig. 3a).

Microfaults are ubiquitous in some chert packets, restricted to some layers in other packets, and utterly lacking in still other packets. Where well-developed, they segment the chert layers into north–south-trending brittle boudins with rhomboid profiles (Fig. 3a). Identically oriented boudin-like structures that have curved elliptical or lensoidal profiles (Fig. 3b) are believed to have been brittle boudins that were strongly modified by silica dissolution and removal and are called 'solution boudins' (Brueckner & Snyder 1985a). All gradations can be observed between the angular profiles of brittle boudins and the curved profiles of solution boudins.

*Folds*

Asymmetric, east-verging folds in cherts of the Havallah sequence display strikingly variable fold geometries from one packet to another (see figs. 8a–d and 9 in Brueckner & Snyder, 1985a). Tight to isoclinal folds with layers that are thickened at the hinges relative to the limbs (Classes 1C and 2 of Ramsay, 1967) apparently underwent deformation while the chert layers were ductile. Parallel folds (class 1B) formed by flexural slip between layers, suggesting greater competence of the layers. Chevron and box folds commonly have fractured and brecciated hinges indicating some brittle behavior during folding. Still other folds are actually composed of layers that have been dismembered brittly into rotated and translated chert blocks that are internally unfolded. A few chert packets lack folds entirely and may have been too rigid to deform. These variations in fold style can be attributed to a host of causes such as differences in temperature, stress, strain rate, pore fluid pressure and so on. However, where these variations are observed within single layers or between layers of the same fold, it seems more likely that the different structural responses represent differences in the properties of the layers themselves.

The hinge area of a folded layer containing mound structures (Fig. 3c) illustrates ductility variations within single layers. Four small mounds (labeled M) show little evidence of internal strain whereas the matrix is highly contorted.

Figure 3(d) shows an example of a strong ductility contrast between two adjacent layers of the same fold. A competent buckled layer is pulled apart along its outer arc to form V-shaped tension gashes. The gashes are intruded by the more ductile siliceous material from the adjacent layer. The inner arc of the stiffer layer contains clay-rich surfaces that parallel the axial surface of the fold. Contraction along the inner arc caused the removal of material from the right limb by pressure solution.

Another example of different folding mechanisms in neighboring layers of the same megascopic fold is shown in Fig. 4(a). The hinge of the upper chert layer (Figs. 4a & b) has an irregular profile cut by a network of clay-rich solution cleavage surfaces that, on average, parallel the fold axial surface. The laminae that outline the fold are straight between the cleavage surfaces, but show abrupt angle changes at the surfaces. The hinge in the next layer (Figs. 4a & c) shows a smoothly curved profile interrupted by only a few solution cleavage surfaces and micro-fractures. Pressure solution appears to have played a dominant role in the formation of the hinges of the upper layer whereas the lower layer folded by buckling and flexural slip along thin bedding-parallel microstylolite seams.

*Dilation structures*

Quartz and chalcedony-filled crack–seal fractures, hydraulic fractures, dilation breccias and clastic sills and dikes are locally abundant in the Havallah sequences (Brueckner & Snyder 1985a). Most dilation structures cross-cut or brecciate solution boudins and associated microstylolites. One clastic sill occupies a thrust fault and another intrudes solution boudins (Brueckner & Snyder 1985a, fig. 13). These structures therefore indicate that one or more episodes of high pore-fluid pressure occurred during main phase thrusting and folding of the allochthon.

## DISCUSSION

Significant rheological and solubility variations occur in Havallah cherts on the interpacket, interlayer and intralayer scale. We propose that these differences can be explained if the chert was deformed while it was undergoing silica diagenesis. This deformation–diagenesis model was introduced in another paper (Snyder *et al.* 1983) for the largely siliceous Miocene Monterey Formation of California. The Monterey Formation is sufficiently young to continue to preserve siliceous sediments in different diagenetic states. Structures within the different diagenetic zones of the Monterey Formation serve as modern-day analogues for interpreting structures in the Havallah sequence. The proposed comparisons cannot be exact. The Monterey Formation formed largely from the deposition of diatom frustiles whereas the siliceous portions of the Havallah sequence formed from radiolaria tests: differences in porosity, permeability, ductility and so on are inevitable. The tectonic environments differed for the two sequences and it is unreasonable to expect structures to be identical. The Havallah sequence has completely converted to quartzose rocks; there is no *a priori* way of knowing the diagenetic state of siliceous packets of this sequence when they were deformed. This last point is particularly bothersome since some of the variations we have described can be explained by causes other than differences in diagenetic state. For example, pressure-solution rates can be influenced by variations in clay content (Marshak & Engelder 1985) or by differences in grain size (Williams *et al.* 1985). Despite these problems, the relationship between structural style and diagenetic state in the Monterey Formation provides a model that can be applied instructively to the interpretation of structures in older siliceous assemblages such as the Havallah sequence.

*Silica diagenesis*

We assume that most of the siliceous sediments of the Havallah sequence were initially radiolarian oozes with varying amounts of terrigeneous detritus (clay being dominant). The biogenic silica in siliceous organisms is amorphous, relatively open-structured, hydrous opal (opal-A, terminology of Jones & Segnit 1971). Opal-A remains stable during the early phases of burial and lithification. Diatom oozes lithify to form *opaline-diatomaceous sediments* (or *diatomites*) and radiolarian oozes form *opaline radiolarian sediment*. Upon deeper burial, the silica in these weakly cemented sediments dissolves and reprecipitates as a mixed polymorph of cristobalite and tridymite called opal-CT. Opal-CT bearing sediments are called *CT-porcelanites* if they are clay-rich and porous or *CT-cherts* if they are clay-poor and relatively non-porous. Further burial causes the silica to undergo a second solution–reprecipitation reaction to from quartz and the resultant rocks are *quartz-cherts* if they are clay-poor and *siliceous argillites* (or *quartz-porcelanites*) if they are richer in clay. These reactions generally occur at low temperatures (<50°C; Pisciotto 1981a) in deep sea sediments.

The silica polymorphic transitions result in large volume changes as progressively denser silica phases form and porosity decreases from nearly 80% for diatomites to less than 10% for quartz cherts (Hamilton 1976, Isaacs 1981). The reactions also cause the expulsion of large amounts of crystallographically-bound water since opal-A and opal-CT contain up to 20 and 13 weight % water, respectively (Keene 1976, Jones & Segnit 1972, Hurd & Thayer 1977). Finally the solubility of silica in water decreases very sharply in the sequence opal-A $\rightarrow$ opal-CT $\rightarrow$ quartz under otherwise identical conditions (Kastner 1979, Williams *et al.* 1985).

The driving forces for the silica reactions are the solubility of the different polymorphs in aqueous solutions and particle surface area (Williams *et al.* 1985). Rates are controlled primarily by temperature, hence the time span between and during each silica phase transition is a function of burial depth and local geothermal gradient. Total time for diagenetic conversion to the quartz stage may be as short as 4–12 million years for thick continental margin deposits such as the Monterey Formation, where rapid burial to high temperatures accelerated the dissolution and reprecipitation reactions (Pisciotto 1981a, Williams *et al.* 1985). On the other hand, tens of million years may be required for phase changes in low temperature deep-sea deposits of low sedimentation rates (Hein *et al.* 1981a & b, Pisciotto 1981b). The chemistries of both pore fluids and sediments also control the rate of diagenetic reactions (Williams & Crerar 1985). Clays retard the rate of conversion of opal-A to opal-CT whereas Mg-bearing carbonates accelerate it (Kastner *et al.* 1977 and references therein, Isaacs 1982). Conversely, the presence of clay in opal-CT siliceous sediments may accelerate their conversion to quartz (Isaacs 1982). The control exerted by clays is important to our model.

Depths and thicknesses of diagenetic zones in the Monterey Formation vary from a few tens of m to several hundred m (Pisciotto 1981a, Issacs, 1982). The boundaries between the diagenetic zones are gradational and contain layers that are in different diagenetic states as a result of different initial chemistries. These mixed zones may be several tens of m thick (Snyder *et al.* 1983).

*Pressure-solution features*

Under otherwise identical conditions, the abundance of pressure-solution features should decrease in the sequence opaline radiolarian sediment > CT-porcelanite > CT-chert > quartz-chert as a result of the decreasing porosity of the sediment (and hence decreasing water/rock ratios) and the decreasing solubility of the silica polymorphs with advancing diagenesis. The Havallah sequence itself provides the best evidence for the model. Pressure solution features are generally lacking within mound structures, relative to the surrounding matrix (Figs. 2c and 3c). By analogy with morphologically similar CT-chert nodules within diatomite in the Monterey Formation (Fig. 5), Havallah mounds probably were at one time nodules that were in a higher diagenetic state than the surrounding matrix. Silica conversion to the next polymorph starts along a series of points of favorable composition within certain siliceous beds (Pisciotto 1978, Jenkyns & Winterer 1982, Hein *et al.* 1981a). Conversion continues concentrically outward from these nuclei, sometimes generating the growth rings such as those found in both Havallah mounds (Fig. 2d) and Monterey nodules (Fig. 5a). We propose that loading-induced bed-parallel pressure solution began while the Havallah sediments were in this nodular configuration and microstylolites developed preferentially in the more soluble matrix. Where dissolution and silica removal were intense the microstylolites formed swarms and seams that preserved the nodular fabric by accreting against and refracting around the less soluble nodules.

The process outlined above either created or radically accentuated a contrast in clay content between matrix and mounds. A bed that may have had a more or less uniform clay content along strike parallel to mound development became a layer with alternating clay-rich (matrix) and clay-poor (mounds) zones along strike after pressure solution.

The interplay betwen silica solubility and silica diagenesis is illustrated most clearly in a Havallah mound shown in Fig. 2(d) where microstylolites are systematically more abundant towards the margin. One explanation for this fabric is that the mound grew at the same time that the microstylolites were forming. Microstylolites are rarer in the core because their development was arrested early when the nucleus converted to a less soluble state of silica. Microstylolites continued to develop in the soluble matrix surrounding the nucleus until they were fossilized by the growing nodule. They are most abundant at the margin because the silica there was in a lower diagenetic state longer than at the core. The clear mound at the top of the photo may have converted to an advanced diagenetic state very early and hence contains no microstylolites.

We propose a related mechanism to explain the thin argillite–thick chert couplet so characteristic of the Havallah sequence and other ribbon cherts (Jenkyns & Winterer 1982). Clay-rich beds remain in the opal-A diagenetic state longer than adjacent clay-poor layers, which convert relatively rapidly to opal-CT (Isaacs 1982). The result can be the alternating layers of different diagenetic states that are so characteristic of much of the Monterey Formation. If the sequence is loaded while the layers are diagenetically mixed, the clay-rich opal-A layers would experience greater pressure solution than adjacent clay-poor opal-CT. The removal of silica would cause the opal-A layers to thin and become even more enriched in a clay residue. The opal-CT layers would experience less, if any, silica removal and remain relatively thick and clay-poor. There is even evidence from the Monterey Formation that the clay-content of opal-CT layers can become further diluted by the introduction of silica into pore spaces (Brueckner & Snyder 1985b). Thus, very small initial differences in clay content can become greatly exaggerated by a pressure solution–silica precipitation process.

There is evidence that contrasts in intralayer and interlayer solubility persisted in Havallah sequence siliceous rocks during layer-parallel shortening ($D_2$ and later). The mounds in the hinge area shown in Fig. 3(c) contain few pressure-solution features whereas the matrix contains abundant, cross-cutting microstylolites and clay-rich seams. The matrix appears to have become contorted and dissolved by pressure solution during deformation while the mounds merely rotated and translated and underwent little or no internal strain or dissolution. Similarly, the upper layer shown in Fig. 2(b) underwent more shortening by pressure solution than the lower layer. The clay seam between the layers acted as a décollement allowing the two layers to behave independently.

It is not clear, however, whether the continued existence of these solubility contrasts during tectonism reflects the persistence of diagenetically mixed layers, or whether it simply reflects variations in some other factor. Clays, for example, may exert the same controls on dissolution rates in cherts as they do in limestones (Marshak & Engelder 1985). Clay-rich layers could develop pressure-solution features more readily than clay-poor layers even though all layers are in the quartzose state. This possibility is difficult to evaluate because of ambiguities in cause and effect. Microstylolites are indeed most abundant in clay-rich layers of the Havallah sequence, but they are clay-rich, at least in part, because silica removal has enriched the layers in residual clay. Furthermore, clay helps retard the conversion of opal-A to opal-CT, thereby keeping clay-rich layers in lower diagenetic states longer than neighboring clay-poor layers. Thus, except for the case of the mound structures, it is not generally obvious whether clay-rich layers developed pressure-solution features preferentially because they were in lower diagenetic states or because they were clay-rich or because of both factors.

The evidence cited for the mound structures suggests that variations in the degree of pressure solution were induced by differences in diagenetic state early in the evolution of Havallah siliceous sediments. At the very least, this early process exaggerated small primary differences in clay content and thereby influenced later clay-controlled variations in dissolution rates.

If, as we propose, diagenetically mixed zones persisted during tectonism, they provide a ready model for explaining the boudin-like fabric ($D_1$ in Table 1) of some Havallah cherts (see Fig. 6). Brittle behavior would be

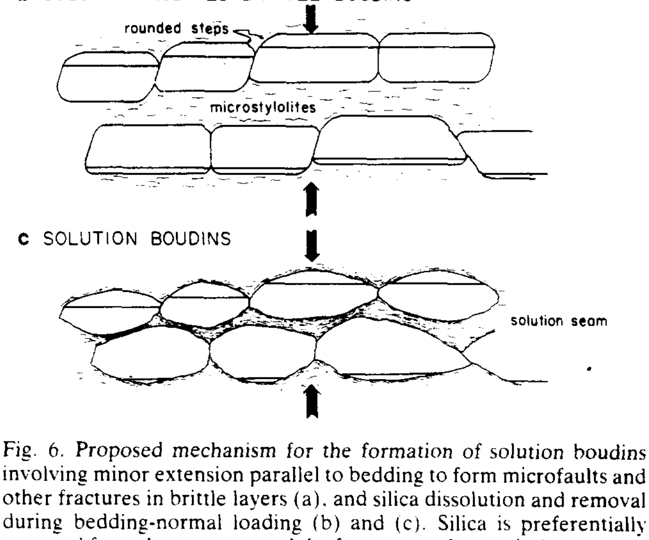


Fig. 6. Proposed mechanism for the formation of solution boudins involving minor extension parallel to bedding to form microfaults and other fractures in brittle layers (a), and silica dissolution and removal during bedding-normal loading (b) and (c). Silica is preferentially removed from the areas around the fractures to form solution 'necks'. Compare with Figs. 3 (a & b).

expected if some layers were CT- or quartz-chert whereas adjoining ductile layers in lower diagenetic states could extend uniformly. The north–south-striking microfaults and other fractures that bound brittle boudins tend to be restricted to individual clay-poor chert layers and do not extend into the thin intervening argillaceous layers. Either the clay-rich layers were too ductile to fracture, and extended instead by flow, or the evidence for the fractures was obliterated as the clay-rich layers thinned by further bed-parallel pressure solution. The microfaults provided pathways for fluids and exposed new surface areas for dissolution. The angular steps at the intersection of bedding and step planes must have been particularly vulnerable to silica removal. We propose that silica removal around the fractures rounded the steps and locally thinned the layers to produce solution 'necks' (Fig. 3b), whereas the unfractured areas between the necks had less silica removed and remained thick. The north–south preferred orientation of the solution necks is the result of the preferred orientation of the microfaults. The simultaneous dissolution of the intervening clay-rich layers (Fig. 6) formed microstylolite swarms and seams that molded themselves around the lensoid profiles of the relatively less soluble solution boudins.

### *Folds*

Folds within the Monterey Formation display heterogeneous styles, even within single outcrops (see figs. 4, 5 and 6 in Snyder *et al.* 1983). These variations can often be ascribed to rheological differences caused by differences in diagenetic states. Monterey folds that clearly involved ductile flow occur largely in diatomites (Fig. 5b). Pore-fluid pressures in the porous, yet relatively impermeable diatomites (Hamilton 1976, Isaacs 1982), appear to have been sufficiently high that diatom frustiles and frustile fragments became decoupled and could move by each other (a sort of intergranular slip) during folding. Chert layers from the Havallah sequence that show clear evidence of intralayer flow are thought to have formed through an analogous mechanism, while the layers were still opaline radiolarian sediments or perhaps CT-porcelanites. Radiolarian tests within these folds are rarely distorted, and appear also to have resisted dissolution since microstylolites tend to wrap around them. Evidence from Deep-Sea Drilling Project cores shows that the shells of radiolaria and other microfossils commonly convert to quartz much sooner than the matrix (Hein *et al.* 1981b). If so radiolaria would tend to resist internal deformation during folding, and prove to be unsuitable passive strain indicators.

The Monterey Formation contains numerous box, chevron and parallel folds, usually in layers composed of CT-porcelanite and CT-chert. CT-chert layers are locally tightly folded by upright, irregularly-spaced buckle folds enclosed in diatomite that is unfolded (see figs. 4c–e in Snyder *et al.* 1983). The stiff CT-chert layer accommodated layer-parallel shortening by buckling whereas the enclosing diatomite shortened without folding. Folded CT-chert and CT-porcelanite zones in the Monterey Formation are associated with thrust faults, structures that are rare in the more ductile diatomites. The transition of opal-A to opal-CT seems to result in siliceous layers that are sufficiently strong to buckle and/or fault rather than deform by intralayer flow. We postulate that analogous transitions occurred in the Havallah sequence resulting in the formation of the chevron and parallel folds that characterize the $D_2$ fabric (Table 1).

It is entirely possible that flexural slip folds could not have developed in the Golconda allochthon until bed-parallel solution processes had formed the argillite seams between chert layers. Where slip cannot occur at the contacts between beds the rocks will fault (Johnson 1980). The argillite seams between most Havallah chert layers appear to have acted as such interlayer décollements (see Fig. 2b) either because of their high, diagenetically-enhanced clay-content or because of high pore-fluid pressures (Johnson & Page 1976) generated in these layers as a result of silica dehydration reactions.

Monterey folds associated with diagenetically advanced rocks (CT-cherts, quartz-porcelanites and especially quartz-cherts) are typically associated with brittle features including faults, fractures and breccias. Hinges in thin-layered quartz-chert, particularly, are commonly defined by curved trains of brecciated fragments that are internally unfolded (Fig. 5d, see also fig. 6d in Snyder *et al.* 1983). The fragments are held together by tar, carbonate or silica cements. Where they are cemented by silica, the hinges present the false impression of being smoothly folded when viewed from a distance. Folds with tension gashes, brecciated hinges, faulted hinges and other brittle features (Fig. 3d) in the Golconda allochthon are suggested to have formed in similar diagenetically advanced rocks.

Some Havallah chert packets are unfolded. Perhaps they were too thick and too strong to bend as a result of being uniformly diagenetically mature. For example, folds are scarce in bedded jaspers and jasperoids in the immediate vicinity of the Big Mike Mine (a massive sulfide body) in the northern Tobin Range (Snyder 1977, 1978). Hydrothermal activity associated with the formation of Big Mike may have converted associated cherts to the quartzose state early so that the cherts faulted and brecciated rather than folded during deformation.

### *Dilation structures*

Thrust faults, hydraulic fractures, veins filled with carbonate, silica or tar, dilation breccias, clastic dikes and other dilation structures are very common in brittle siliceous rocks of advanced diagenetic states in the Monterey Formation (Roehl 1981, Redwine 1981, see figs. 6b–e and 7c in Snyder *et al.* 1983). Roehl (1981) presents a detailed model for the formation of dilation breccias in the Monterey Formation involving the natural hydraulic fracturing of pre-existing fracture networks as a result of excess pore-fluid pressures.

We propose that the dehydration of opal-A and opal-CT to form anhydrous quartz can create or at least contribute to episodes of high pore-fluid pressure within siliceous sediments. High pore-fluid pressures would be especially likely if the siliceous sediments have the very low permeabilities that characterized the diatomites of the Monterey Formation (Isaacs 1981) since fluids will not be able to escape freely when the rocks are subjected to burial and/or tectonic compression (Carson *et al.* 1982). These episodes in turn are very likely to lead to the formation of brittle dilation structures in siliceous sediments since silica diagenesis also results in progressively more brittle and less porous rocks.

Many of the dilation structures of the Havallah sequence clearly formed during deformation (Brueckner & Snyder 1985a, see figs. 12, 13) especially during the formation of the $D_2$ fabric (Table 1). The syntectonic diagenesis of silica provides a relatively simple way of explaining episodes of high pore-fluid pressure during deformation. The anomalously high pore-pressure could have further influenced deformation by dilating potential thrust surfaces so that faulting could occur. This process would explain why the many thrust faults that bound tectonic packets of the Golconda allochthon lack appreciable brecciated zones. High pore-fluid pressure, and the possible persistence of diagenetically-immature ductile siliceous sediments, may have created décollements that caused thrusting to be relatively aseismic. Unfolded ribbon chert packets may have escaped internal deformation as a result of decoupling along these décollements.

## CONCLUSIONS

We have argued (Brueckner & Snyder 1985a) that the packet fabric of the Golconda allochthon in the areas we have studied records a very large amount of shortening, and that the multiple structural events that preceded, accompanied and postdated the development of some tectonic packets argue for a prolonged structural evolution. These observations can be fitted to an accretionary prism-obduction model for the structural evolution of the Golconda allochthon as has been advocated by Dickenson (1977), Speed (1977b), Schweickert & Snyder (1981) and Snyder & Brueckner (1983). Here we propose that siliceous sediments become progressively more brittle and less soluble as a result of processes that accompany silica diagenesis, and that these changes provide a general mechanism for explaining the variable development and heterogeneous geometries of folds and other structures in the Havallah sequence. If we are correct, the diagenesis–deformation model offers further support for the long-lived accretionary prism model.

Evidence that siliceous sediments were in variable diagenetic states at the time they were deformed is recorded in siliceous packets of all ages in the Havallah sequence: upper Devonian–lower Mississippian cherts display the same fabrics and structural heterogeneity as upper Permian cherts (Brueckner & Snyder 1985a). If deformation were restricted entirely to the Permo-Triassic Sonoma orogeny, the older siliceous sediments should have approached, if not completed, diagenesis as a result of: (1) deep burial by upper Mississippian, Pennsylvanian and Permian clastic and siliceous sediments; and (2) the long interval of time (*ca* 100 million years) between deposition and tectonism. Tectonism should have resulted in relatively brittle deformation for old chert packets, and ductile deformation and pressure solution-rich features should be restricted to the relatively thin veneer of young, diagenetically immature siliceous sediments. These arguments would be particularly true if the Havallah sequence was thick and/or deposited in a basin of high heat flow, such as a back-arc basin (Burchfiel & Davis 1975, Miller *et al.* 1982) since both of these factors would accelerate silica conversion rates.

On the other hand, an accretionary prism associated with long-lived subduction would be fed a continuous supply of diagenetically mixed siliceous sediments some of which were deposited in front of the prism shortly before they were intercalated. Several recent studies of such prisms (Nelson 1982, Speed & Larue 1982, Speed 1983) document the presence of early ductile folds. These structures are attributed to deformation of recently deposited, weakly lithified sediments that were rapidly incorporated into the prism (Nelson 1982, Lundberg & Moore 1982, Speed 1983). This same conveyor-belt process can introduce older, more deeply buried, and hence more lithified sediments into the prism, which would deform in a more brittle and insoluble fashion.

Some of the oldest chert packets (Late Devonian–Early Mississippian) display ductile, solution-rich tectonic structures implying that they were diagenetically immature during deformation. We suggest these sediments were deformed within a few tens of millions of years after deposition. Thus we argue for the existence of an active accretionary wedge relatively early in the upper Paleozoic; a prism that remained active until it was thrust or obducted over western North America during the Permo-Triassic Sonoma orogeny.

*Acknowledgements*—This manuscript is the combined result of field work by Hannes Brueckner and Walter Snyder during the summers of 1979 and 1980 and a Queens College of CUNY Masters Dissertation on polished slabs and thin sections of Havallah cherts by Marion Boudreau. Ken Coles, Bill Devlin, Steve Goldstein, Afsar Sachi and Marion Boudreau made important contributions as field assistants.

The authors thank Ian Dalziel, Steve Marshak, Bob Turner, Steve Bachman, Jim Helwig, an unnamed reviewer, and especially Elizabeth Miller for constructively criticizing earlier versions of this manuscript, Joan Totton for patiently typing several versions, and Mary Ann Luckman for her technical help and drafting. Bob Speed, Susan Laule, Elizabeth Miller, Greg Davis, Dave Rodgers and many others have tried to keep us honest about interpreting the Golconda allochthon structural fabric. Carolyn Isaacs, Ken Pisciotto, James Hein and Charlotte Schreiber helped us learn the intricacies of silica diagenesis. The work was supported by NSF grants EAR-78-23585, EAR-79-05722 and EAR-79-11301. Lamont–Doherty contribution number 4122.

## REFERENCES

Brueckner, H. K. & Snyder, W. S. 1985a. Structure of the Havallah sequence, allochthon, Nevada: evidence for prolonged evolution in an accretionary prism. *Bull. geol. Soc. Am.* **96**, 1113–1130.

Brueckner, H. K. & Snyder, W. S. 1985b. Chemical and Sr-isotopic variations during diagenesis of Miocene siliceous sediments of the Monterey Formation, California. *J. sedim. Petrol.* **55**, 553–568.

Burchfiel, B. C. & Davis, G. A. 1975. Nature and controls of Cordilleran orogenesis, western United States: extensions of an earlier synthesis. *Am. J. Sci.* **275A**, 363–396.

Carson, B., von Huene, R. & Arthur, M. 1982. Small-scale deformation structures and their physical properties related to convergence in Japan Trench slope sediments. *Tectonics* **1**, 277–302.

Dickinson, W. R. 1977. Paleozoic plate tectonics and the evolution of the Cordilleran continental margin. In: *Paleozoic Paleogeography of the Western United States*, Pacific Coast Paleogeography Symposium 1 (edited by Stewart, J. H., Stevens, C. H. & Fritsche, A. E.). *Spec. Publs Soc. Econ. Paleontol. Mineral.* 137–156.

Ferguson, H. G., Roberts, R. J. & Muller, S. W. 1952. Geology of the Golconda Quadrangle, Nevada. *Quad. Map U.S. geol. Surv.* (GQ-15).

Hamilton, E. L. 1976. Variations of density and porosity with depth in deep sea sediments. *J. sedim. Petrol.* **46**, 280–300.

Hein, J. R. & Jsueh-Wen Yeh. 1981a. Oxygen-isotope composition of chert from the mid-Pacific Mountains and Hess Rise, Deep-Sea Drilling Project Leg 62. *Initial Rept Deep-Sea Drill. Proj.* **62**, 749–758.

Hein, J. R., Vallier, T. L. & Allan, M. A. 1981b. Chert petrology and geochemistry, mid-Pacific Mountains and Hess Rise, Deep-Sea Drilling Project Leg 62. *Initial Rept Deep-Sea Drill. Proj.* **62**, 711–748.

Hurd, D. C. & Thayer, F. 1977. Changes in the physical and chemical properties of biogenic silica from the central equatorial Pacific: part II—refractive index, density, and water content of acid cleansed samples. *Am. J. Sci.* **277**, 1168–1202.

Isaacs, C. M. 1981. Porosity reduction during diagenesis of the Monterey Formation, Santa Barbara Coastal Area, California. In: *The Monterey Formation and Related Siliceous rocks of California* (edited by Garrison, R. E. & Douglass, R. G.). *Spec. Publs Soc. Econ. Paleontol. Mineral. Pacific. Sec.* 257–272.

Isaacs, C. M. 1982. Influence of rock composition on kinetics of silica phase changes in the Monterey Formation, Santa Barbara area, California. *Geology* **10**, 304–308.

Jenkyns, H. C. & Winterer, E. L. 1982. Palaeoceanography of Mesozoic ribbon radiolarites. *Earth Planet. Sci. Lett.* **60**, 351–375.

Johnson, A. M. & Page, B. M. 1976. Development of folds within Huasna Syncline, San Luis Obispo County, California. *Tectonophysics* **33**, 97–143.

Johnson, A. M. 1980. Folding and faulting of strain hardening sedimentary rocks. *Tectonophysics* **62**, 251–278.

Jones, J. B. & Segnit, E. R. 1971. The nature of opal. I. Nomenclature and origin of constituent phases. *J. geol. Soc. Aust.* **18**, 57–68.

Kastner, M., Keene, J. B. & Gieskes, J. M. 1977. Diagenesis of siliceous oozes. I. Chemical controls on the rate of opal-A diagenesis—an experimental study. *Geochim. cosmochim. Acta* **41**, 1041–1059.

Kastner, M. 1979. Silica polymorphs. In: *Mineralogical Soc. Am. Short Course Notes: Marine Minerals* (edited by Burns, R. G.), **6**, 99–107.

Keene, J. B. 1976. Distribution, mineralogy, and petrography of biogenic and authigenic silica in the Pacific Basin. Unpublished Ph.D. thesis, University of California, San Diego, Scripps Institute of Oceanography.

Laule, S. W., Snyder, W. S. & Ormiston, A. R. 1981. Willow Canyon Formation, Nevada: an extension of the Golconda allochthon. *Abs. Prog. geol. Soc. Am.* **13**, 66.

Lundberg, N. & Moore, J. C. 1982. Brittle versus ductile forearc areas: synthesis of macroscopic structural features from DSDP cores. *Abs. Prog. geol. Soc. Am.* **14**, 551.

Marshak, S. & Engelder, T. 1985. Development of cleavage in limestone of a fold-thrust belt in eastern New York. *J. Struct. Geol.* **7**, 345–359.

Miller, E. L., Holdsworth, B. K., Whiteford, W. B. & Rodgers, D. 1984. Stratigraphy and structure of the Schoonover complex, northeastern Nevada: implications for Paleozoic plate-margin tectonics. *Bull. geol. Soc. Am.* **95**, 1063–1076.

Nelson, K. D. 1982. A suggestion for the origin of mesoscopic fabric in accretionary melange, based on features observed in the Crystalls Beach Complex, South Island, New Zealand. *Bull. geol. Soc. Am.* **93**, 625–634.

Pisciotto, K. A. 1978. Basinal sedimentary facies and diagenetic aspects of the Monterey Shale, California. Unpublished Ph.D. thesis, University of California, Santa Cruz.

Pisciotto, K. A. 1981a. Diagenetic trends in the siliceous facies of the Monterey shale in the Santa Maria region, California. *Sedimentology* **28**, 547–571.

Pisciotto, K. A. 1981b. Distribution, thermal histories, isotopic compositions and reflection characteristics of siliceous rocks recovered by the Deep Sea Drilling Project. In: *The Deep Sea Drilling Project, A decade of Progress* (edited by Warme, J. E., Douglass, R. G. & Winterer, E. L.). *Spec. Publs Soc. Econ. Paleontol. Mineral.* **32**, 129–148.

Ramsay, J. G. 1967. *Folding and Fracturing of Rocks*. New York, McGraw-Hill.

Redwine, L. E. 1981. Hypothesis combining dilation, natural hydraulic fracturing and dolomitization to explain petroleum reservoirs in Monterey Shale, Santa Maria Area, California. In: *The Monterey Formation and Related Siliceous Rocks of California* (edited by Garrison, R. E. & Douglass, R. G.). *Spec. Publs Soc. Econ. Paleontol. Mineral. Pacific. Sec.* 221–248.

Roberts, R. J., Hotz, P. E., Gilluly, J. & Ferguson, H. G. 1958. Paleozoic rocks of north-central Nevada. *Bull. Am. Ass. Petrol. Geol.* **42**, 2813–2857.

Roehl, P. O. 1981. Dilation brecciation—a proposed mechanism of fracturing, petroleum expulsion and dolomitization in the Monterey Formation, California. In: *The Monterey Formation and Related Siliceous Rocks of California* (edited by Garrison, R. E. & Douglass, R. G.). *Spec. Publs Soc. Econ. Paleontol. Mineral. Pacific Sec.* 285–316.

Rye, R. O., Roberts, R. J., Snyder, W. S., Lahusen, L. G. & Motica, J. E. 1984. Textural and sulfur isotopic studies of Big Mike cupriferous volcanogenic massive sulfide deposits, Pershing County, Nevada. *Econ. Geol.* **79**, 124–140.

Schweickert, R. A. & Snyder, W. S. 1981. Paleozoic plate tectonics of the Sierra Nevada and adjacent regions. In: *The Geotectonic Evolution of California, A Symposium in Honor of W. W. Rubey* (edited by Ernst, W. G.), Prentice-Hall, New York, 182–201.

Siever, R. 1983. Evolution of chert at active and passive continental margins. In: *Siliceous Deposits of the Pacific Region* (edited by Iijma, A., Hein, J. & Siever, R.). *Develop. Sedimentol.* **36**, 7–24.

Silberling, N. J. & Roberts, R. J. 1962. Pre-Tertiary stratigraphy and structure of northwestern Nevada. *Spec. Pap. geol. Soc. Am.* **72**, 1–58.

Snyder W. S. 1977. Origin and exploration for ore deposits in Upper Paleozoic chert-greenstone complexes of northern Nevada. Unpublished Ph.D. thesis, Stanford University.

Snyder, W. S. 1978. Manganese deposited by submarine hot springs in chert–greenstone complexes, western United States. *Geology* **6**, 741–744.

Snyder, W. S. & Brueckner, H. K. 1983. Tectonic evolution of the Golconda allochthon, Nevada: problems and perspectives. In: *Paleozoic and Early Mesozoic Rocks in Microplates of Western North America* (edited by Stevens, C. A.). *Spec. Publs Soc. Econ. Paleontol. Mineral., Pacific. Sec.* 103–123.

Snyder, W. S., Brueckner, H. K. & Schweickert, R. A. 1983. Deformation styles in the Monterey formation and other siliceous sedimentary rocks. In: *Petroleum Generation and Occurrence in the Miocene Monterey Formation, California* (edited by Isaacs, C. M. & Garrison, R. E.). *Spec. Publs Soc. Econ. Paleontol. Mineral. Pacific. Sec.* 151–170.

Speed, R. C. 1977a. An appraisal of the Pablo Formation of presumed Late Paleozoic age, central Nevada. In: *Paleozoic Paleogeography of the Western United States*, Pacific Coast Paleogeography Symposium 1 (edited by Stewart, J. H., Stevens, C. H. & Fritsche, A. E.). *Spec. Publs Soc. Econ. Paleontol. Mineral., Pacific. Sec.* 315–324.

Speed, R. C. 1977b. Island-arc and other paleogeographic terranes of Late Paleozoic age in the western Great Basin. In: *Paleozoic Paleogeography of the Western United States*. Pacific Coast Paleogeography Symposium 1 (edited by Stewart, J. H., Stevens, C. H. & Fritsche, A. E.). *Spec. Publs Soc. Econ. Paleontol. Mineral. Pacific. Sec.* 349–363.

Speed, R. C. 1983. Structure of the accretionary complex of Barbados, I: Chalky Mountain. *Bull. geol. Soc. Am.* **94**, 92–116.

Speed, R. C. & Larue, D. K. 1982. Barbados: architecture and implications for accretion. *J. geophys. Res.* **87**, 3633–3643.

Stewart, J. H., MacMillan, R. R., Nichols, K. M. & Stevens, C. H.

1977. Deep-water upper Paleozoic rocks in north-central Nevada—a study of the type area of the Havallah Formation. In: *Paleozoic Paleogeography of the Western United States*. Pacific Coast Paleogeography Symposium 1 (edited by Stewart, J. H., Stevens, C. H. & Fritsche, A. E.). *Spec. Publs Soc. Econ. Paleontol. Mineral. Pacific. Sec*. 337–347.

Stewart, J. H., Murchey, B., Jones, D. L. & Wardlaw, B. W. 1986. Paleontologic evidence for complex tectonic interlayering of Mississippian to Permian deep water rocks of the Golconda allochthon in the Tobin Range, north-central Nevada. *Bull. geol. Soc. Am.* **97**, 1122–1132.

Wanless, H. R. 1979. Limestone response to stress: pressure solution and dolomitization. *J. sedim. Petrol.* **49**, 437–462.

Williams, L. A., Parks, G. A. & Crerar, D. A. 1985. Silica diagenesis, I. Solubility controls. *J. sedim. Petrol.* **55**, 301–311.

Williams, L. A. & Crerar, D. A. 1985. Silica diagenesis, II. General mechanisms. *J. sedim. Petrol.* **55**, 312–321.